Scaling Method for Force Feedback of Forceps Manipulator Based on Beam Theory

S. Maeda, K. Oiwa, and C. Ishii
Hosei University, Tokyo, Japan
Email: shotaro.maeda.ku@stu.hosei.ac.jp, c-ishii@hosei.ac.jp

Abstract— **In this study, a new scaling method for force feedback is proposed for the surgical robot developed in our laboratory, incorporating an analysis of the shaft of the forceps based on beam theory. A six-axis force and torque sensor is attached to the base parts of the forceps manipulator of the surgical robot to detect a force applied at the tip or shaft part of the forceps. Then, the detected force is amplified using the proposed scaling method and the amplified force is realized through the haptic device Omega 7. Experiments were conducted to verify the effectiveness of the proposed scaling method. The results showed that the operator of the surgical robot can experience a small force that was applied to the forceps more clearly and quickly compared with that realized when the conventional constant scaling method is used.**

Index Terms—**forceps manipulator, force feedback, haptic device, scaling method, beam theory, force and torque sensor**

I. Introduction

Minimally invasive surgery requires accurate and delicate operation in a small workspace and a limited field of vision, requiring considerable surgical skill. Starting with the first operation over a hundred years ago, the field of laparoscopic surgery has significantly developed recently due to the development of new techniques as well as various surgical robots which are proposed in Ref. [1]-[3]. The da Vinci robot developed by Intuitive Surgical Inc. is currently the most advanced surgical robot. This is a master–slave robot with plural robot arms, stereoscopic imaging by the 3D endoscope, and manipulators that imitate the movement of human wrist with seven degrees of freedom (DOF) by the wire drive. Moreover, Ref. [4] described that single-port surgery (SPS) has gained significant popularity with the increasing development of laparoscopic surgery in recent years. This procedure is more cosmetically favorable than the conventional laparoscopic surgery. Unfortunately, the use of surgical robots for SPS has still not been practical. Reference [5] described SPS that was conducted using the da Vinci robot by replacing manipulators with those with the SPS's capable shape; however, this robot is not yet in practical use. Furthermore, medical accidents have been reported during laparoscopic surgery using the da Vinci robot because the robot is unable to provide force feedback to the surgeons. As discussed in Ref. [6]-[8] force feedback is known to have many benefits such as the improvement of the surgeon's dexterity and the enhancement of the operability of surgical robots in telesurgery.

To solve this issue of the current surgical robots, in this study, a six-axis force and torque sensor produced by ATI Co. is attached on an independently developed SPS forceps manipulator. The sensor detects an external force at the tip or shaft of the forceps manipulator, enabling the realization of force feedback by using haptic function of the Omega 7 master device developed by Force Dimension Co. Moreover, a new scaling method of the haptic function is proposed to enable the improvement of the performance of the force feedback in various laparoscopic surgical robots beyond the SPS robot. Specifically, the operator of the surgical robot clearly experiences a small force by the proposed scaling method based on the beam theory for realizing feedback of the force detected by the sensor.

II. Laparoscopic Surgery and Single-Port Surgery

Laparoscopic surgery is a surgical technique in which a laparoscope and forceps are inserted into 1-2 cm incision holes opened on the abdominal surface of the patient and performed while observing the laparoscopic image on the monitor. SPS is a laparoscopic surgery procedure that has seen a rapid spread in recent years. This technique is different from the conventional laparoscopic surgery in that one incision hole is made by the scalpel at only the umbilicus part of the patient for mounting an exclusive port, whereas laparoscopic surgery is performed by inserting two dedicated forceps and one laparoscope into the hole. In the conventional laparoscopic surgery, the incision holes are made by the scalpel in 3-6 locations on the patient's body to insert the laparoscope and forceps. SPS has a high cosmetic value because it does not leave a surgical scar because of the integrated nature of the procedure as the scalpel is placed only on the umbilicus of the patient. As discussed in Ref. [9], the low risk of post-surgery complications is an additional advantage of SPS. Fig. 1 shows a schematic illustration of the SPS.

Manuscript received November 17, 2015; revised January 17, 2016.

doi: 10.18178/ijpmbs.5.1.23-30

III. Forceps Manipulator for SPS

A. Forceps Manipulator and Robot Arms for SPS

Reference [10] has demonstrated the development of the forceps manipulator for conventional laparoscopic surgery, which can be remotely operated with an independently developed master device for realizing force feedback. Furthermore, a forceps manipulator for SPS has been developed in Ref. [11] by remodeling the ready-made SPS forceps, with the same manipulations of rotation, grasping, and bending of the tip part moved by the motor drive. In this case, the Omega 7 that is a seven-DOF haptic device developed by Force Dimension Co. is the master device, the developed forceps manipulator is the slave device, and the forceps manipulator is remotely operated by controlling its tip position by the master–slave control. The specifications for the developed forceps manipulator are as follows.

1) *Rotation:* The rotational motion at the tip of the forceps is remotely operated by the motor drive.
2) *Grasping:* The open-and-close motion of the grasping at the tip of forceps is remotely operated by the motor drive.
3) *Bending:* The omnidirectional bending motion at the tip of the forceps is remotely operated by the motor drive.

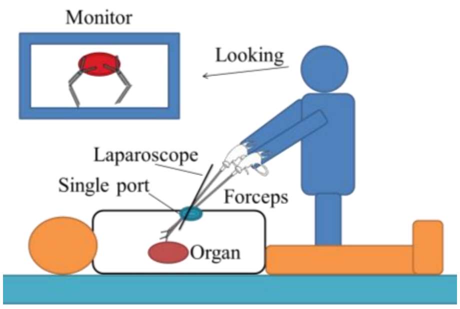

Figure 1. Single-port surgery (SPS).

Fig. 2 shows the independently developed robot arms for SPS. The developed forceps manipulator is mounted on the arm of the SPS robot because it cannot be used alone as a surgical robot. In a different approach, a new surgical tool arrangement called rotation arrangement in SPS was evaluated in Ref. [12]. These robot arms have been designed for the realization of the rotation arrangement. These robot arms can move the developed forceps manipulator with three DOF of yaw, pitch, and translation by the motor drive.

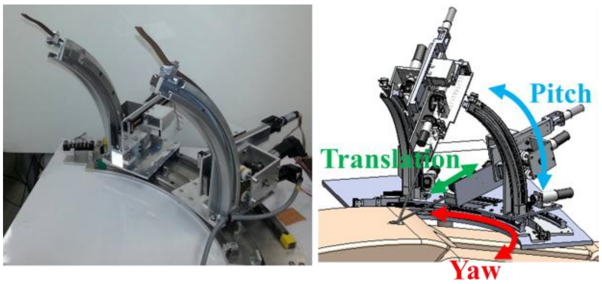

Figure 2. Robot arms for SPS.

The size and mass of the developed forceps manipulator are limited by the ability of the robot arm to support the mounting of the manipulator. Therefore, the manipulator must be designed keeping in mind this consideration. Fig. 3 shows the developed forceps manipulator. In Fig. 3, the mechanisms of the rotational, grasping, and bending motions at the forceps tip are shown by (a), (b), and (c), respectively.

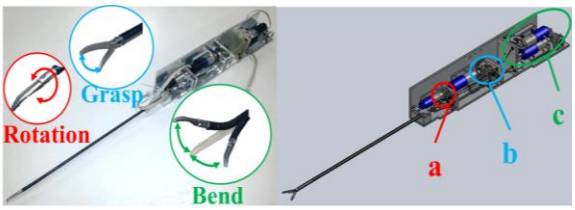

Figure 3. Forceps manipulator for SPS.

B. Master-Slave Control using Omega 7

The SPS forceps manipulator is a slave device, and the haptic device Omega 7 is the master device; therefore, each operation is controlled by the master–slave system, in which the target value of the slave side is calculated from the displacement information of the master side. In this case, a proportional-integral controller is used to construct a tracking control system. Omega 7 is a haptic device that is capable of seven DOF operations: translation motions along the three Cartesian axes, rotary motions around three axes, and the grasping motion along a single axis.

The open-and-close motion of the grasping corresponds to the pinching of the grasping part of Omega 7, the tip rotation corresponds to the rotation around a single upper arm axis of Omega 7, and the bending motion in the vertical and transverse directions corresponds to the up-and-down and left-and-right direction rotations of the operating unit of Omega 7. Fig. 4 shows the operating unit of Omega 7 and the corresponding actions of the developed forceps manipulator.

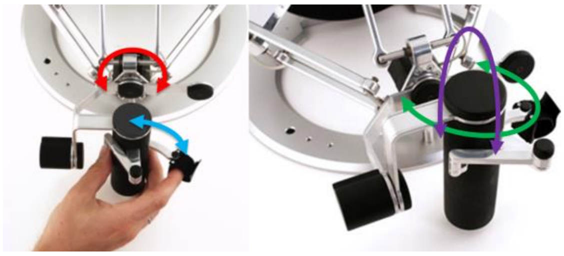

(a) Master device (Omega 7).

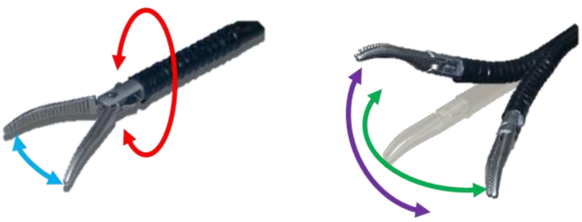

(b) Slave device (forceps manipulator).

Figure 4. Manipulations of Omega 7 and forceps manipulator.

IV. Force Feedback

A. *Force Feedback in Surgical Robot*

Currently, the surgical robots in practical use do not have a force feedback function. Therefore, surgical robots cannot transmit the senses of touching or holding objects with the tip of the forceps manipulator to the operating surgeon. Reports on medical accidents that caused organ damage due to lack of the force feedback function exist. Therefore, the development of force feedback has become a key problem in the development of surgical robots. The desirable feedback forces in laparoscopic surgery or SPS with a surgical robot are the grasping force when organs are grasped with the forceps tip, the contact force when the organs are touched with the tip, and the pressure force when organs are pressed with the shaft. Reference [13] has already reported the development of force feedback for the grasping force. Therefore, this study focuses on the development of the feedback of the force added to the tip or shaft of forceps. A six-axis force and torque sensor Mini40 produced by ATI Co. is attached to the root portion of the previously developed SPS forceps manipulator and is used to detect the external force added to the forceps' tip or shaft. The detected sensor value is then transmitted to the robot operator through Omega 7, which is the input device with the force feedback function, thus realizing the feedback of the force added to the forceps. Fig. 5 shows the corresponding forces for the sensed force on the forceps manipulator and force feedback to Omega 7. An external force along the three axes of the forceps shaft is realized on the three orthogonal axes of Omega 7.

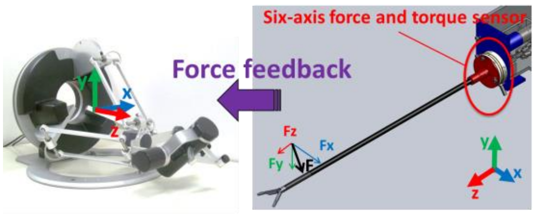

Figure 5. Force sensing and its realization in Omega 7.

B. *Attachment of the 6-axis Force and Torque Sensor Mini40*

Fig. 6 shows a general view of the six-axis force and torque sensor Mini40 produced by ATI Co. and the directions of measurable force and torque. This sensor can detect forces on three orthogonal axes and rotational torques for each axis added to the measurement surface.

In Ref. [14], a six-axis force and torque sensor is attached to the tip of forceps for detecting the external force. However, this is not best choice since insertion of electric sensor into the abdominal cavity is not desirable due to the safety reason.

In our system, since Mini40 has a hole in the center, it can be attached to the root portion of forceps through the shaft in that hole. Therefore, the external force added to the tip or shaft of forceps can be detected without inserting electric sensors into the patient's body. Fig. 7 shows the attachment view of the six-axis force and torque sensor. A cylindrical part (green) is pressed into a disk-like part (red), and these parts are attached to the measurement surface of the Mini40 through the forceps shaft in the sensor's center hole. Mini40 is fixed at the root portion of the manipulator shaft with an angle-shaped part (blue) and a plate-like part (purple).

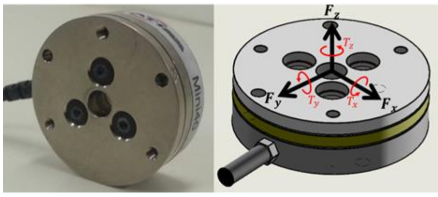

Figure 6. Mini40 and measurable force and torque

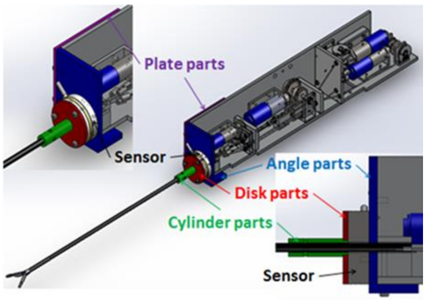

Figure 7. Attachment of six-axis force and torque sensor.

C. *Force Detection Using Six-axis Force and Torque Sensor*

We verified that the force added to the tip or shaft of forceps was actually detected with the six-axis force and torque sensor. An external force was applied several times to the forceps tip in the horizontal direction (*x*-direction is *Fx*), the vertical direction (*y*-direction is *Fy*), and the shaft direction (*z*-direction is *Fz*) with the finger. Figs. 8, 9, and 10 show the detected results for each direction. Inspection of these figures indicates that detection of the *Fx* and *Fy* components of the force added to forceps was stable; however, *Fz* was not detected stably. Detection of the force for the shaft direction was difficult because the attachment parts of six-axis force sensor were fixed at the forceps shaft only at the screwing point in the mounting structure, leading to deviation in the detected force value for the applied shaft direction force. It is investigated that the detected sensor value does not necessarily return to zero for *Fx*, *Fy*, and *Fz* results, returning to the unloaded state after a single application of an external force. This indicates the occurrence of drift in the force detection by some of the strain gauges built into the sensor.

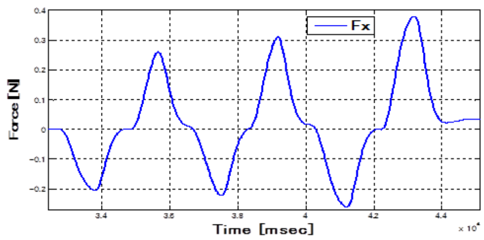

Figure 8. Force sensing in *x* direction.

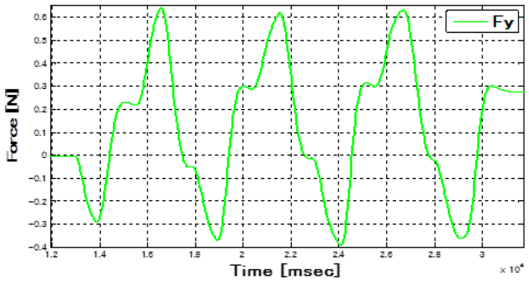

Figure 9. Force sensing in *y* direction.

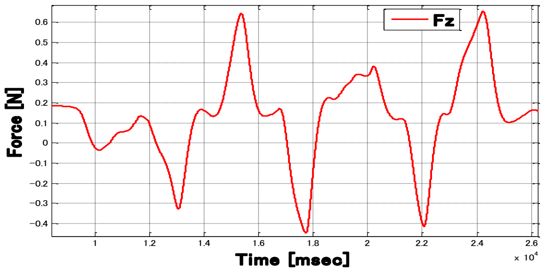

Figure 10. Force sensing in *z* direction.

V. Force Scaling

A. Scaling of Force for Force Feedback

The *Fx* and *Fy* values detected stably by the six-axis force and torque sensor were directly fed back to the robot operator through Omega 7. However, the operator could not recognize the force well because the value of the force detected by the sensor was small. Therefore, the detected value of *Fx* and *Fy* are scaled up a magnitude that can be recognized by the operator and displayed in Omega 7.

If the detected sensor value is multiplied by a large constant value, the operator can recognize the force even if the detected force is small. However, this may adversely affect the surgical operation because the force feedback is too strong then. Thus, it is necessary to scale the force up to a magnitude for which the robot operator can recognize even a small detected value without adversely affecting the surgical operation.

Therefore we used beam theory to calculate the deflection amount of the forceps shaft due to the applied external force. Furthermore, we proposed a method for scaling up the small detected value for the force applied by the touch of the tip or shaft of the forceps, using the dynamics of the forceps tip by the external force. Thereby the detected sensor value increases rather than constant multiple, while ensuring that the value is not sufficiently large to adversely affect the surgical operation. The following configurations are used for the proposed scaling method.

Configuration I): The shaft of forceps manipulator is considered a cantilever, and the deflection and deflection angle are calculated.

Configuration II): The motion equation of the mass point at the tip of the cantilever when the external force is added to the tip is considered.

Configuration III): The motion equation of Omega 7 corresponding to the motion equation in the configuration II is introduced, and the force value realized by Omega 7 is calculated.

In the configuration I, the shaft of forceps manipulator is divided into a cylindrical stainless steel section, which is the shaft of the remodeled original SPS forceps and a cylindrical aluminum section attaching the six-axis force and torque sensor on the forceps manipulator. Next, the shaft of the forceps manipulator is considered as two connected cantilevers, assuming the screwing point that fixes the cylindrical stainless steel part and the cylindrical aluminum part, and the portion attaching the sensor are the fixed ends. It is assumed that a concentrated load is only added to the cantilever tip. Fig. 11 shows the model for which the shaft of forceps manipulator is assumed to be the cantilever. The *x*-direction deflection on the *x*-*z* plane and the *y*-direction deflection on the *y*-*z* plane are considered in the same manner, because the cross-sectional shape of the cantilever is a hollow circle.

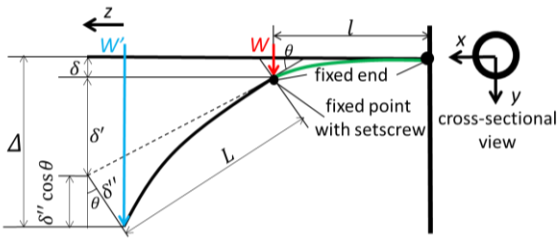

Figure 11. Cantilever beam model of shaft of forceps manipulator.

In Fig. 11, *w* is the value detected by the six-axis force and torque sensor (*Fx* or *Fy*). Since the load added to the cantilever is constant for all positions of the cross-section, the following relationship is established for *w* and *w*′.

$$W = W' \ , \tag{1}$$

where l is the distance of the fixed end from the point fixed with screw on the aluminum part attaching the force and torque sensor, E_{Al} is the longitudinal elastic modulus of aluminum part, and I_{zp} is the geometrical moment of inertia. The deflection δ and deflection angle θ of the cylindrical aluminum part are given by (2) and (3).

$$\theta = -\frac{Wl^2}{2E_{Al}I_{zp}} \tag{2}$$

$$\delta = \frac{Wl^3}{3E_{Al}I_{zp}} \tag{3}$$

L is the distance from the point fixed with the screw on the aluminum part to the forceps tip and δ' is given by (4).

$$\delta' = L\sin\theta \tag{4}$$

E_f is the longitudinal elastic modulus of the cylindrical stainless steel part that is the shaft of the remodeled original forceps, I_{zf} is the geometrical moment of inertia, and the deflection δ'' is given by (5).

$$\delta'' = \frac{W'L^3}{3E_fI_{zf}} \tag{5}$$

Then, the deflection Δ of the cantilever model in Fig. 11 is given by (6).

$$\Delta = \delta + \delta' + \delta'' \cos\theta \tag{6}$$

In the configuration II, it is assumed that there is a mass point of mass m on the tip of the cantilever model in Fig. 11. The motion of this mass-point when the force f is added to the mass-point is considered as the movement of mass-spring-damper system in which a damper and a combined spring linked to two different springs in series are connected to the mass-point m. Fig. 12 shows the motion model for mass-spring-damper system of the cantilever in Fig. 11.

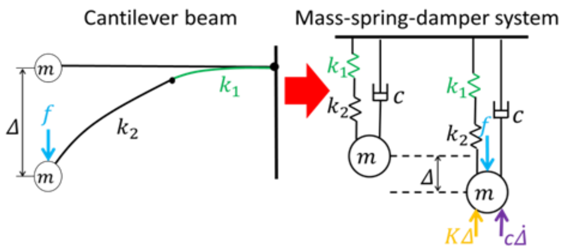

Figure 12. Mass-spring-damper model of cantilever beam.

In Fig. 12, spring constants (flexural rigidity) k_1 and k_2 are calculated using l, E_{Al}, I_{zp}, L, E_f, and I_{zf} by the following equation.

$$k_1 = \frac{3E_{Al}I_{zp}}{l^3} \quad , \quad k_2 = \frac{3E_f I_{zf}}{L^3} \tag{7}$$

Furthermore, since the two springs are connected in series, the combined spring constant K of k_1 and k_2 is given by the following equation.

$$K = \frac{k_1 k_2}{k_1 + k_2} = \frac{E_{Al}E_f I_{zp} I_{zf}}{E_{Al}I_{zp}L^3 + E_f I_{zf} l^3} \tag{8}$$

Moreover, it is assumed that the model of mass-spring-damper system in Fig. 12 does not vibrate by critical damping. Therefore, the damping coefficient c of the damper is expressed by following equation because the damping ratio is 1.

$$c = 2\sqrt{mK} \tag{9}$$

The motion equation for the mass-spring-damper system in Fig. 12 is given by the following equation.

$$f - K\Delta - c\dot{\Delta} = m\ddot{\Delta} \tag{10}$$

In the configuration III, the motion equation of (10) is applied to the master device Omega 7. For operating the SPS robot, the displacement Δ and the mass m are replaced respectively by the operation amount λ of Omega 7 and the mass M of forearm of operating human. The motion equation of the operating unit in Omega 7 is then given by the following equation

$$F - K\lambda - C\dot{\lambda} = M\ddot{\lambda} \quad , \tag{11}$$

where F is the force which Omega 7 should realize. Fig. 13 shows the model for the motion model of mass-spring-damper system in Fig. 12 which is adapted to Omega 7.

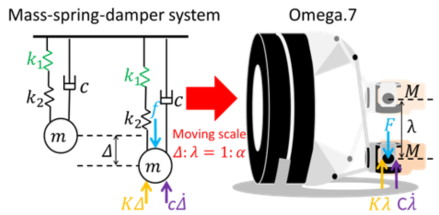

Figure 13. Application of mass-spring-damper model to Omega 7.

In the motion equation of operating unit in Omega 7 of (11), the unit is assumed not to vibrate by critical damping as well as the damping expressed by (9). Thus, a coefficient C is given by the following equation.

$$C = 2\sqrt{MK} \tag{12}$$

It is also assumed that the ratio of the displacement of the slave side, which is the tip movement displacement of the SPS robot and the displacement of master side, which is the operating amount of Omega 7 (position control magnification rate of the SPS robot) is $1{:}\alpha$, then the displacement of operating unit in Omega 7 λ is expressed by the following equation.

$$\lambda = \alpha\Delta \tag{13}$$

By substituting (13) into (11), the force value F which Omega 7 should realize is derived by (14). Because Omega 7 has a function to ensure gravity when force is applied, the effect due to the weight of the operating unit is not considered.

$$F = M\alpha\ddot{\Delta} + C\alpha\dot{\Delta} + K\alpha\Delta \tag{14}$$

B. Force Feedback to Omega 7

The detected sensor force value was scaled up using the proposed scaling method and compared with the standard constant multiple scaling. A maximum of 1.0 N force was applied several times to the forceps tip in the horizontal direction (*x*-direction) and the vertical direction (*y*-direction) with the finger. Fig. 14 shows a graph of scaled force in the horizontal direction (*x*-direction), Fig. 15 shows a graph of scaled force in the vertical direction (*y*-direction); the detected sensor force value, the scaled value obtained by the proposed scaling method and the scaled value obtained using a constant multiple (two times) are shown in both figures. Since the mass of human forearm is about 3.1% of body weight, the mass M of the forearm was 2.17 kg as the weight of the operator was 70 kg. The ratio of the displacement of slave side to the displacement of master side was 1:2, and the value of F was calculated for $\alpha = 2$.

The data presented in Figs. 14 and 15 do not exhibit large differences between the scaled sensor values obtained using a constant multiple and the scaled values obtained by the proposed scaling method. However, since the feedback force to the operator obtained by the proposed scaling method considers the dynamics (deflection) generated by the load added to the forceps shaft, it is considered that the proposed scaling method can provide force feedback to the operator more clearly and quickly for the small value than the normal constant multiple scaling when the applied force varies rapidly. The value for which humans can recognize the force is approximately 1 N. Henceforth, the superiority of the proposed scaling method is verified by applying a force that can be noticed by humans and changing a speed of the force.

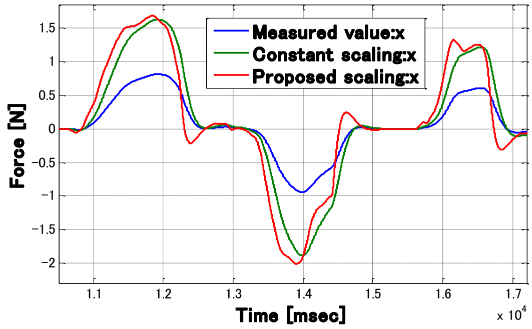

Figure 14. Scaling of force in *x* direction.

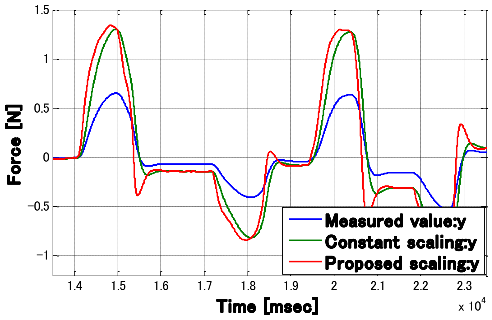

Figure 15. Scaling of force in *y* direction.

C. *Advantageous Validation of Scaling Method*

The following simulations were performed to verify the superiority of the proposed scaling method. When the force imitating the detected sensor value was gradually increased from 0 to 0.5 N, the difference indicated was simulated in the proposed scaling method and the normal constant multiple (two times) scaling. The times for reaching the maximum force of 0.5 N are simulated for the three time intervals of 1.0 s (Slow), 0.50 s (Intermediate), and 0.25 s (Quick). The mass M of the forearm was 2.17 kg, the ratio of operating amount of Omega 7 to the forceps tip movement displacement of the SPS robot, α was 2.

Figs. 16, 17, and 18 show the simulation results for time until the detected sensor value reached 0.5 N in the case of 1.0, 0.50, and 0.25 s.

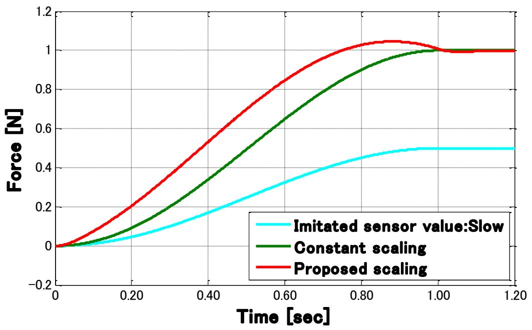

Figure 16. Simulation result (Slow).

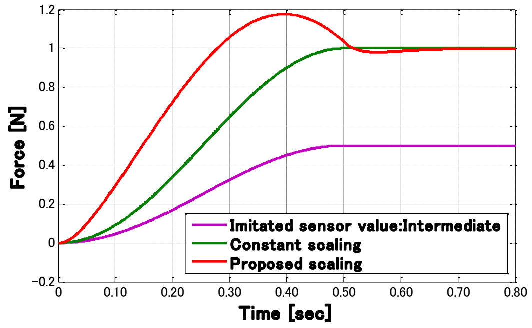

Figure 17. Simulation result (Intermediate).

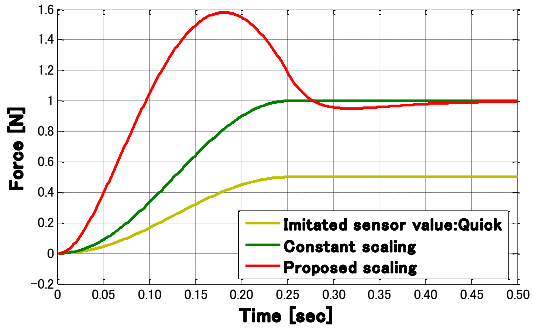

Figure 18. Simulation result (Quick).

In Figs. 16, 17, and 18, as the time interval of the force imitating the detected sensor value becomes small, response of the proposed scaling method becomes quick as compared with that of the constant multiple scaling. Moreover, the maximum value scaled by the proposed method is larger than constant multiple scaling. Therefore, in the scaling using the proposed method, when the amount of change of the detected sensor value per unit time is increased, the maximum scaled value becomes large. Since it is possible to strongly feedback the operator to the force variation when touched with the tip or shaft of forceps, the operator can clearly and quickly experience the small force detected by the sensor using the proposed method.

D. *Advantage Validation Experiment of Scaling Method*

The SPS robot was moved periodically by sinusoid input in horizontal direction, which was the "yaw" direction in Fig. 2, the tip of forceps manipulator was hit to a building block such that the detected sensor value of the horizontal direction (x-direction) was approximately 0.5 N. Next, this force was fed back to the subject who held the operating unit of Omega 7. During this experiment, the subject was not given visual information; however, only force information was given. Then, when the tip of forceps manipulator hit the building blocks, the time until the subject experienced the force feedback was measured using a stopwatch. Furthermore, using the proposed scaling and constant multiple scaling methods, experiments were performed 10 times each in 2 subjects. Fig. 19 shows the scenario of the experiment.

The measurement times with constant multiple scaling and with proposed scaling were compared. Table I. shows the measurement times of each subject. Fig. 20 shows a graph of detected sensor value of the horizontal direction (x-direction), the value scaled up with constant multiple (two times), and the value using the proposed scaling method.

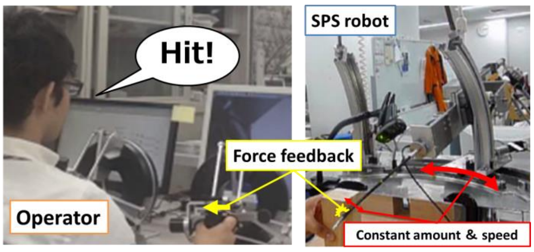

Figure 19. Experiment for verification of superiority.

TABLE I. EXPERIMENTAL RESULTS

	Subject A		Subject B	
Number of times	Constant scaling [sec]	Proposed scaling [sec]	Constant scaling [sec]	Proposed scaling [sec]
1	4.51	3.68	4.85	2.58
2	7.90	3.80	4.22	2.93
3	5.68	3.81	5.09	2.43
4	7.05	2.30	5.41	3.23
5	4.73	2.85	4.67	2.27
6	6.61	3.23	4.46	3.19
7	7.20	3.05	4.90	3.30
8	7.93	3.11	4.79	3.26
9	6.61	2.55	4.33	4.24
10	4.90	2.78	4.75	3.52
Average	**6.31**	**3.12**	**4.75**	**3.10**

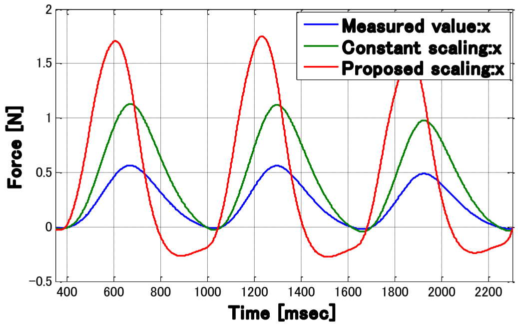

Figure 20. Comparison of scaling of force.

Table I. indicates that both subject, A and B, recognize the force quicker using the proposed method than the constant multiple scaling when the tip of forceps manipulator hit the building block. In Fig. 20, it is indicated that the maximum value of the force using the proposed scaling method is larger than constant multiple scaling.

Therefore, the proposed scaling method can transmit the force more quickly than constant multiple scaling method. Moreover, the robot operator can clearly experience the small force, since the proposed scaling method can feedback strongly the force.

VI. CONCLUSION

In this study, a six-axis force and torque sensor was attached in the root of the independently developed forceps manipulator for SPS. Then, the external force added to the tip or shaft of forceps was detected, and force feedback was conducted to the robot operator through Omega 7. The added force of horizontal and vertical directions can be detected stable. However, the force of shaft direction cannot be detected stably.

The forceps shaft was assumed as cantilever, the movement by external force added to the cantilever tip is replaced by the operating unit of Omega 7, and it is proposed as a new scaling method, in which the detected force added to the tip or shaft of forceps in horizontal and vertical directions, is scaled up and fed back to the operator. Since the dynamics of the forceps shaft was considered, the small detected sensor force value could be fed back more quickly and strongly to the operator using this scaling method compared with that of the constant multiple scaling.

As future challenges, it is raised that the external force in the shaft direction should be detected stably, scaled up using the proposed scaling method, and fed back to the operator through Omega 7. Other than that, a system which removes an interference force caused by the SILS port should be constructed when performing the forceps operation using the SILS port.

REFERENCES

[1] C. Direkwatana, J. Suthakorn, and C. Wilasrusmee, “Development of wire-driven laparoscopic surgical robotic system, MU-LapaRobot,” *Proceedings of IEEE International Conference on Robotics and Biomimetics*, 2011, pp. 485-490.

[2] G. Fau, T. Matsunaga, and K. Ohnishi, “Development of a five degrees of freedom Master/Slave robot for tele-operated laparoscopic surgical operations,” *Proceedings of 7th international Conference on Human System Interactions*, 2014, pp. 172-177.

[3] R. Se-gon, et al., “Development of the SAIT single-port surgical access robot slave arm based on RCM Mechanism,” *Proceedings of 37th Annual International Conference of the IEEE, Engineering in Medicine and Biology Society*, 2015, pp. 5285-5290.

[4] Inderbir S. Gill, et al., “Consensus statement of the consortium for laparoendoscopic single-site surgery,” *Surg Endosc*, vol. 24, pp. 762-768, 2010.

[5] M. Kroh, K. El-Hayek, S. Rosenblatt, B. Chand, P. Escobar, J. Kaouk, and S. Chalikonda, “First human surgery with a novel single-port robotics system: Cholecystectomy using the da Vinci Single-Site platform,” *Springer Science+Business Media*, Surg Endosc, vol. 25, pp. 3566-3573, 2011.

[6] F. Cavallo, G. Megali, S. Sinigaglia, O. Tonet, and P. Dario, “A biomechanicalanalysis of surgeon’s gesture in a laparoscopic virtual scenario,” *Stud. Health Technol. Inf.*, vol. 119, pp. 79-84, 2006.

[7] M. Mitsuishi, et al., “Force-feedback augmentationmodes in the laparoscopic minimally invasive telesurgical system,” *IEEE/ASME Trans. Mechatronics*, vol. 12, no. 4, pp. 447-454, 2007.

[8] C. R. Wagner, et al., “The benefit of force feedback in surgery: Examination of blunt dissection,” *Presence: Teleoperators Virtual Environ*, vol. 16, no. 3, pp. 252-262, 2007.

[9] J. D. Raman, J. A. Cadeddul, P. Raol, and A, Rane, “Single-incision laparoscopic surgery initial urological experience and comparison with natural-orifice transluminal endoscopic surgery,” *BJU International*, vol. 101, no. 12, pp. 1493-1496, 2008.

[10] D. Haraguchi, T. Kanno, K. Tadano, and K. Kawashima, “A pneumatically driven surgical manipulator with a flexible distal joint capable of force sensing,” *IEEE/ASME Trans. Mechatronics*, vol. 99, pp. 1-12, 2015.

[11] D. Yamaoka, K. Oiwa, S. Maeda, and C. Ishii, “Development of a surgical robot for single-port surgery and its position tracking control,” *Proceedings of IEEE International Conference on Robotics and Biomimetics*, 2014, pp. 41-46.

[12] H. Kawamura and C. Ishii, “Mechanical analysis of the formation of forceps and scope for single-port laparoscopic surgery,”

Surgical Laparoscopy, Endoscopy & Percutaneous Techniques, vol. 22, no. 4, pp. 168-175, 2012.
[13] Y. Tsukamoto and C. Ishii, "Estimation of the grasping torque of robotic forceps using the robust reaction torque observer," *Proceedings of IEEE International Conference on Robotics and Biomimetics*, 2014, pp. 1650-1655.
[14] U. Seibold, et al., "Prototype of instrument for minimally invasive surgery with 6-axis force sensing capability," *Proceedings of 2005 IEEE Int. Conf. on Robotics and Automation*, 2005, pp. 496-501.

Shotaro Maeda received his BE in Mechanical Engineering from Hosei University, Japan in 2013. Currently, he is a Master Course student at Graduate School of Engineering, Hosei University, Japan. His research interest is in medical robotics.

Katsuaki Oiwa received his BE in Mechanical Engineering from Hosei University, Japan in 2013. Currently, he is a Master Course student at Graduate School of Engineering, Hosei University, Japan. His research interest is in medical robotics.

Chiharu Ishii received his PhD in Mechanical Engineering from Sophia University, Japan in 1997. From 2002 to 2009, he was an Assistant Professor with Kogakuin University. Currently, he is a Professor at the Department of Mechanical Engineering, Hosei University, Japan. His research interests are in medical robotics, assistive technology and robust control. He is a member of JSME, SICE, RSJ, IEEJ and IEEE.